Clim Dyn (2017) 49:1847–1863
DOI 10.1007/s00382-016-3425-8

The impact of tropical intraseasonal oscillation on the summer rainfall increase over southern China around 1992/1993

Jiabao Wang[1,5] · Zhiping Wen[1,3,4] · Renguang Wu[2] · Ailan Lin[6]

Received: 4 December 2015 / Accepted: 24 October 2016 / Published online: 31 October 2016

Abstract A pronounced summer rainfall increase over southern China occurred around 1992/1993. In the present study, the impact of the boreal summer intraseasonal oscillation (BSISO) on this decadal increase is investigated through diagnostic analysis. It is found that the BSISO-induced rainfall increase accounts for approximately 17.4% of the observed decadal rainfall increase, with a primary part coming from changes in the rainfall pattern associated with phases 3–5 of the BSISO. A further analysis reveals that changes in rainfall pattern over southern China are mainly ascribed to changes in spatial structure of anomalous convection associated with interdecadal change in BSISO tracks. Apart from significant influence of changes in BSISO tracks, changes in the frequency of individual active BSISO phases also have considerable influence on the interdecadal change in summer rainfall over southern China. Based on our analysis, the increase in absolute and relative frequency of occurrence of phases 1 and 8, coupled with their corresponding rainfall pattern, makes a positive contribution to the increase in southern China summer rainfall. The interdecadal change in the BSISO tracks and the frequency of active BSISO phases is likely related to coherent changes in atmospheric circulation and sea surface temperature over the Indian Ocean and the western Pacific.

Keywords Intraseasonal oscillation (ISO) · Interdecadal change · Summer rainfall · Southern China

✉ Zhiping Wen
eeswzp@mail.sysu.edu.cn

1 Center for Monsoon and Environment Research and Department of Atmospheric Sciences, Sun Yat-Sen University, Guangzhou 510275, China

2 Center for Monsoon System Research, Institute of Atmospheric Physics, Chinese Academy of Sciences, Beijing 100029, China

3 State Key Laboratory of Severe Weather, Chinese Academy of Meteorological Sciences, Beijing, China

4 Jiangsu Collaborative Innovation Center for Climate Change, Nanjing, China

5 School of Marine and Atmospheric Sciences, Stony Brook University, Stony Brook, NY, USA

6 Key Open Laboratory for Tropical Monsoon, Institute of Tropical and Marine Meteorology, CMA, Guangzhou, China

1 Introduction

Summer rainfall over eastern China experiences multi-scale changes, e.g., interdecadal variation, interannual variation, intraseasonal oscillation, and synoptic variability, among which interdecadal variation has been a concerned topic in previous studies. Many studies have documented a decadal change in summer rainfall over East China around 1992/1993 (e.g., Kwon et al. 2007; Ding et al. 2008; Yao et al. 2008; Ning and Qian 2009; Wang et al. 2009a, b; Wu et al. 2010; Chen et al. 2012) which is characterized by a shift from a tripole pattern to a dipole pattern. As a result of this change, summer rainfall in southern China experienced a striking increase. Strong upward motion and large moisture transport and convergence associated with a significant weakened Asian summer monsoon system tends to contribute to decadal rainfall increase over southern China (Ding et al. 2008). Changes in atmospheric circulation associated with the rainfall changes were identified (Wu et al. 2010). At the lower-level, there exist two anomalous anticyclones: one over the South China Sea (SCS)-subtropical western North Pacific (WNP) and the other over North China-Mongolia. These two anomalous anticyclones jointly result

in anomalous moisture convergence over southern China, leading to increased rainfall there. Apart from documented interdecadal changes in atmospheric circulation, changes in typhoon tracks might also contribute to interdecadal increase in summer rainfall over southeastern China (Kwon et al. 2007; Chen et al. 2012).

Although a number of studies have made endeavors to analyze causes and mechanisms for the summer rainfall change around 1992/1993 over southern China, most of them focused primarily on interannual or interdecadal timescale. Little attention has been paid to contributions of intraseasonal timescale variations so far albeit it has been pointed out summer rainfall in eastern China displays prominent intraseasonal fluctuations (e.g., Lau and Chan 1986; Wang and Xu 1997; Chen et al. 2001; Yang and Li 2003; Mao and Chan 2005). Therefore, it is requisite to discern plausible contributions of intraseasonal oscillations in order to advance the knowledge of possible reasons for this pronounced interdecadal change.

The linkage between tropical intraseasonal oscillation (ISO) and summer rainfall over southern China has received some consideration. Zhang (2013) pointed out that about 50–80% of the total intraseasonal variance in the Asian summer monsoon rainfall is explained by the ISO. Similar finding and detailed descriptions are provided by Goswami (2012) and Hsu (2012). Zhang et al. (2009) proposed two plausible mechanisms for the impact of the Madden–Julian oscillation (MJO) (Madden and Julian 1971, 1972) on summer rainfall in eastern China using daily multivariate MJO index (Wheeler and Hendon 2004). One is that the Rossby wave forced by the MJO located over the Indian Ocean (IO) propagates northeastward along low level westerly waveguide and influences Southeast China, leading to increased rainfall there. The other is that upward branch of anomalous local Hadley circulation moves northward when the MJO enters the western Pacific (WP), which drives eastward retreat of the western Pacific subtropical high (WPSH) and less moisture transport into Southeast China, hence leading to decreased rainfall there. In light of differences in the propagation path between the MJO (referred to boreal winter ISO) and the BSISO (referred to boreal summer ISO) (Wang and Rui 1990; Wang and Xie 1997; Lawrence and Webster 2002; Jiang et al. 2004, etc.), Chen et al. (2014a, b) reexamined the relationship between the BSISO and summer rainfall over southern China using the BSISO index (Kikuchi et al. 2012) that could better capture the northward movement of ISO. As the ISO itself experienced an interdecadal change around 1992/1993 (Kajikawa et al. 2009), the relationship between the BSISO and summer rainfall over southern China incurred an interdecadal change accordingly (Kajikawa and Wang 2012). After 1993, summer rainfall over southern China received much more influence from intraseasonal convection

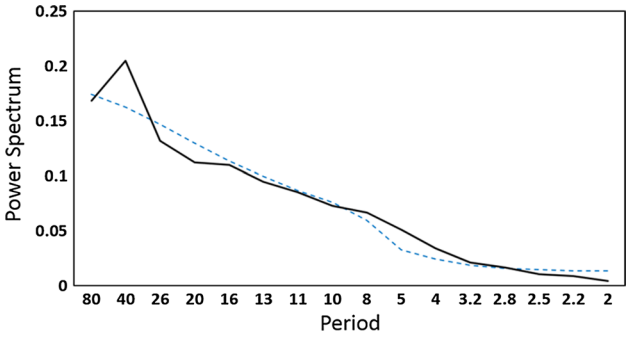

Fig. 1 20 year-mean (1983–2002) power spectrum of summer rainfall variation averaged over southern China (100°–125°E, 20°–30°N) (*solid black line*). Also shown is the 90% confidence upper limits of red noise spectrum (*dashed blue line*). 25–90 days and 2–8 days are found as prominent oscillation periods of southern China summer rainfall variation

anomalies over the SCS while it was mainly affected by anomalies over the northern IO before 1993. A recent study also pointed out significant decadal changes in the BSISO around 1998 and 2008 (Yamaura and Kajikawa 2016). BSISO activity during 1999–2008 was enhanced compared to that during 1984–1998; meanwhile, the northward propagation was reduced in latter period. But the above mentioned situation changed its sign during 2009–2014. The impact of ISO on tropical and extratropical mean field (i.e., precipitation, surface temperature, etc.) has been detected in some previous studies (Ferranti et al. 1990; Higgins and Mo 1997; Mutai and Ward 2000; Lawrence and Webster 2001; Yoo et al. 2011, 2012a, b; Lee et al. 2011a, b). The above studies shed light on impacts of ISO on summer rainfall on both intraseasonal and interdecadal timescales.

Previous studies motivate us to raise several questions: (1) what's the relative contribution of decadal change in intraseasonal summer rainfall over southern China to total summer rainfall; (2) to what extent could the BSISO cast influence on interdecadal change of summer rainfall over southern China and (3) through which ways? These topics are worthy of investigation since (1) southern China summer rainfall experiences dominant intraseasonal fluctuation (Fig. 1) which implies a contribution of decadal change in intraseasonal summer rainfall to the observed significant increase in southern China summer rainfall; (2) BSISO is active in summer and has large influence on southern China summer rainfall (Zhang et al. 2009; Kajikawa and Wang 2012; Chen et al. 2014a, b, etc.) which alludes its role in changing intraseasonal southern China summer rainfall and hence changing mean rainfall; (3) the integral effect (upscale feedback) of shorter timescale variation to longer timescale has been suggested in previous studies (Zhou et al. 2006; Kwon et al. 2007; Yoo et al. 2011, 2012a, b; Kajikawa and Wang 2012, Chen et al. 2012, etc.); (4) under

the modulation impact of changes in large-scale circulation accompanying the southern China summer rainfall increase (Ding et al. 2008; Wu et al. 2010), the direct impact of same-scale variation (in this case, change in the BSISO) on intraseasonal summer rainfall may provide some useful information of observed southern China rainfall increase. In this study, the contribution of the BSISO-induced rainfall change to the interdecadal change of southern China summer rainfall around 1992/1993 is separated into two parts: changes in intraseasonal rainfall anomalies associated with the spatial structure of the BSISO, and those associated with the frequency of active BSISO phases.

The organization of this article is as follows: Introductions to the datasets and methods are provided in the next section. The interdecadal change in summer rainfall over southern China is examined in Sect. 3. The impact of the BSISO on discerned interdecadal change of summer rainfall around 1992/1993 is discussed in Sect. 4 along with the potential mechanism. A summary is given in Sect. 5, and discussion is provided in Sect. 6.

2 Datasets and methods

In the present study, for cross validation, we used two sets of precipitation data to analyze the interdecadal change in southern China summer rainfall. One is daily gridded precipitation dataset provided by China Meteorological Data Sharing Service System with horizontal resolution of 0.5° longitude × 0.5° latitude. The other is daily rainfall dataset of 752 stations in China provided by the National Climate Center of the China Meteorological Administration. The former set of precipitation data is interpolated onto grids using Thin Plate Spline (TPS) based on the latter precipitation dataset and has been proved to have high precision according to the assessment provided by the National Climate Center.

The daily mean interpolated outgoing longwave radiation (OLR) data derived from the National Oceanic and Atmospheric Administration (NOAA) with a spatial resolution of 2.5° is used as a proxy of anomalous convection associated with the BSISO. The daily BSISO index defined by Kikuchi et al. (2012) is used, which could be obtained from the website (http://iprc.soest.hawaii.edu/users/kazuyosh/Bimodal_ISO.html), to represent the characteristics of the BSISO. According to Kikuchi et al. (2012), the BSISO could be separated into eight phases, with phases 1–2 corresponding to anomalous convection over the Bay of Bengal, phases 3–4 to strengthened convection over India and the Maritime Continent, phases 5–6 to enhanced convection over the WNP and phases 7–8 to active convection over the eastern North Pacific and equatorial IO. In this study, the active BSISO refers to the amplitude of the BSISO index exceeding 1.5.

The Hadley Centre Sea Ice and Sea Surface Temperature dataset (HadISST) is used in this study, which is available on a 1° × 1° grid, to analyze monthly mean sea surface temperature anomaly (SSTA). We also use monthly mean latent heat flux (positive upward) archived as Objectively Analyzed air-sea Fluxes (OAFlux) dataset for the global oceans. This flux dataset is also available on a 1° × 1° grid.

The reanalysis product used in this study is the European Center Medium-Range Weather Forecasts ERA-Interim reanalysis (Dee and Uppala 2009) on both daily and monthly timescale with a spatial resolution of 0.5° and 1°, respectively. The variables include winds at surface (10 m) and 850 hPa, convergence at 850 hPa.

This study mainly focuses on the boreal summer for the period 1983–2002. Since June to August (JJA) bear similar features in terms of the dominant spatial rainfall pattern and corresponding decadal rainfall change over southern China (figures not shown), JJA mean is used to represent boreal summer. When anchoring intraseasonal timescale, the seasonal cycle was first removed from raw daily data to generate daily anomalies. Then, the Lanczos filter (Duchon 1979) was applied to anomalies to extract the low-frequency signals varying at 25–90 day period.

3 Interdecadal change of summer rainfall over southern China

To better understand how summer rainfall over southern China has changed over past 30 years as a part of eastern China, the dominant modes of summer rainfall variations over eastern China (100°–130°E, 20°–45°N) were extracted first. The empirical orthogonal function (EOF) analysis was applied to unfiltered seasonal (JJA) mean rainfall anomalies derived from the gridded precipitation data for the period 1979–2012. The first two modes explain about 19.5 and 14.8% of the total variance, respectively, which are separable from remaining modes based on the criterion of North et al. (1982). Considering that the percent variances explained by the first two modes are comparable, they should be combined together when examining dominant patterns of eastern China summer rainfall. The spatial distribution and corresponding principal components (PCs) of first two modes are shown in Fig. 2.

The leading EOF mode of summer rainfall anomalies is characterized by a tripole pattern and exhibits significant interdecadal variation with the changing point at 1992/1993, i.e., the leading pattern of eastern China summer rainfall changed from "− + −" to "+ − +" around 1992/1993. As a comparison, the second mode of summer rainfall anomalies reveals a dipole pattern of eastern China summer rainfall and fluctuates mainly on interannual timescale. Nonetheless, a similar interdecadal change in PC2

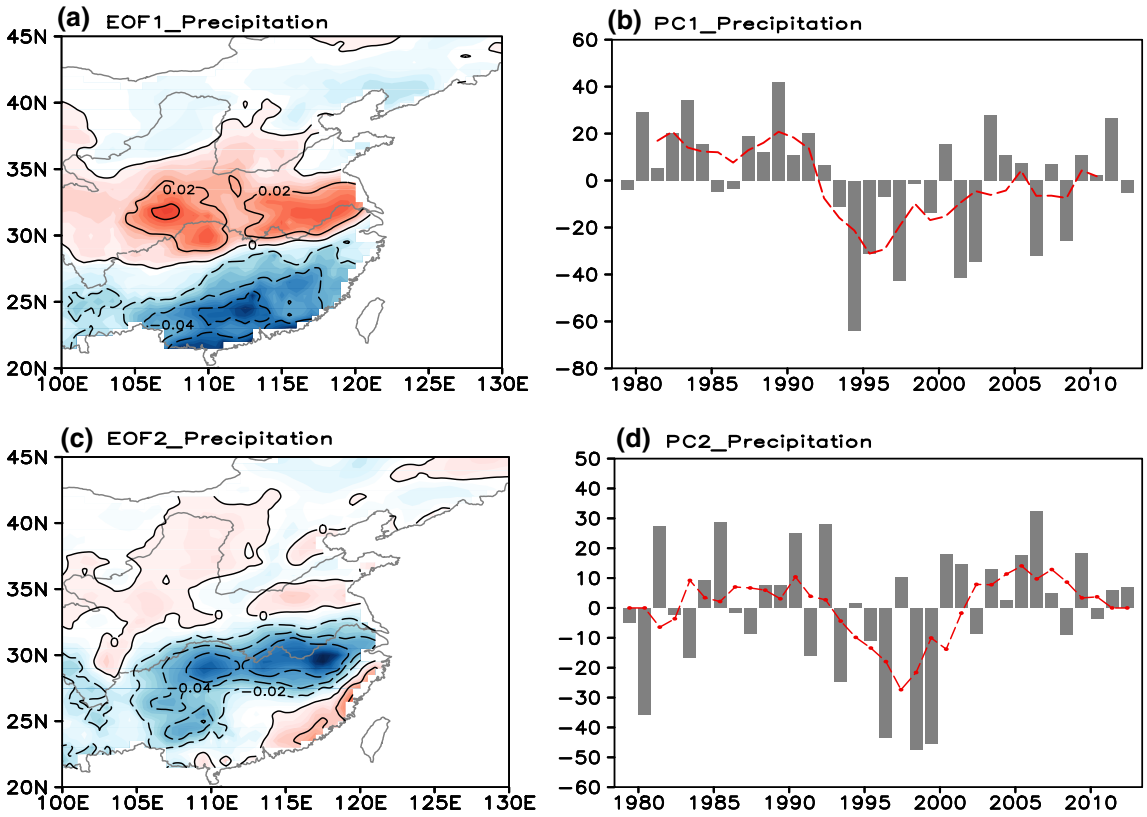

Fig. 2 Spatial pattern of **a** the first and **c** second EOF mode and their corresponding principal components (PCs, *black lines* in **b**, **d**) of the summer rainfall anomalies over East China for the period of 1979–2012. The *red lines* in (**b**), (**d**) represent the 5-year running means of the PCs

could also be discerned around 1992/1993, which reflects the rainfall increase over southern China and decrease over northern China after 1992. In order to examine the significance of interdecadal change discerned in the first two PCs, a 5-year running *t* test was conducted (figure not shown). The results indicate that the values of running *t* test for both PCs exceed the 95% confidence level around 1992/1993.

We constructed a difference of 10-year mean before and after 1992 to depict the spatial distribution of the interdecadal rainfall change. The period before 1983 and after 2002 is excluded in constructing the difference field as large interannual fluctuation is present in PC2 or PC1. The differences derived from the daily gridded precipitation data are shown in Fig. 3. Notable rainfall increase is observed over southern China with the increase up to approximately 2 mm/day, which is consistent with previous studies (e.g., Wu et al. 2010). The 10-year difference of station rainfall data exhibits similar changes, which demonstrates that the results based on gridded precipitation data in this study are credible (figure not shown). The afore-mentioned interdecadal change in summer rainfall over southern China was shown in many previous studies (Ding et al. 2008; Qian and Qin 2008; Yao et al. 2008, etc.). However, the interdecadal change of summer rainfall over southern China from

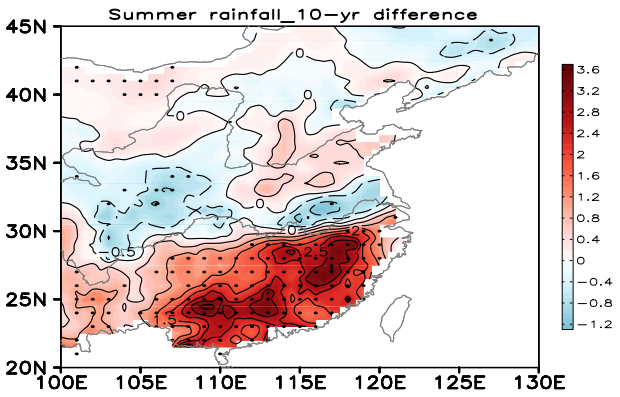

Fig. 3 10-year difference (1993–2002 mean minus 1983–1992 mean) of the eastern China summer rainfall based on gridded data (interdecadal rainfall change, contour interval: 0.5 mm day^{-1}). *Dotted areas* indicate differences exceeding the 95% significance level according to the Student *t* test

perspective of intraseasonal timescale is an overlooked topic. According to the power spectrum analysis (Fig. 1) the dominant variation of southern China summer rainfall is at 25–90 and 2–8 days, and intraseasonal timescale variance accounts for 20.4% to the total variance (figure not

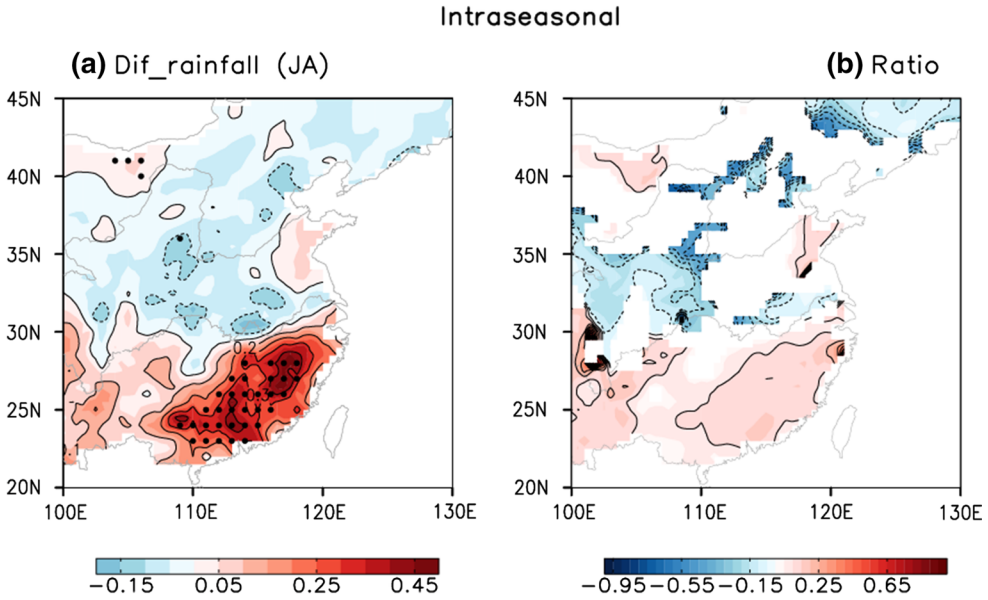

Fig. 4 **a** Same as Fig. 3, but for the 25–90-day filtered precipitation data (contour interval: 0.1 mm day^{-1}). **b** The ratio between panel (**a**) and the observed interdecadal rainfall change (Fig. 3). Values in (**b**) are omitted when the ratio is negative, and the ratio is multiplied by the sign of the corresponding values in (**a**)

shown). The intraseasonal timescale variation will be the main focus in the present study.

4 Impacts of the BSISO on the interdecadal change in southern China summer rainfall around 1992/1993

4.1 Interdecadal change of summer rainfall associated with intraseasonal oscillations

In the last section, a significant interdecadal change in southern China summer rainfall around 1992/1993 is discerned via EOF analysis. Differences of 10-year means revealed a striking rainfall increase over southern China. In this subsection, we will analyze the interdecadal change of southern China summer rainfall from perspective of intraseasonal timescale. The intraseasonal component of summer rainfall anomalies was first extracted using the method described in Sect. 2 and a 10-year difference is then constructed based on filtered rainfall anomalies (Fig. 4a). The spatial distribution of 10-year difference of intraseasonal summer rainfall is reasonably similar to that of raw summer rainfall with less significance in terms of the spatial coverage. Overall, a pronounced increase over the central region of southern China alludes to the importance of intraseasonal timescale variations for the interdecadal rainfall change. Figure 4b shows the ratio between decadal differences of intraseasonal summer rainfall and raw summer rainfall. Generally, the interdecadal change of intraseasonal summer rainfall, to a certain extent, contributes to the interdecadal change in summer rainfall over southern China. The averaged percentage over southern China is about 19.3%.

4.2 Impacts of the BSISO on the interdecadal change

A number of studies have pointed out the important role of ISO in changes of rainfall over Southeast and East Asia (Zhu et al. 2003; Aldrian 2008; Jeong et al. 2008; Tangang et al. 2008; Zhang et al. 2009; He et al. 2011; Jia et al. 2011; Goswami 2012; Hsu 2012), Middle East and South-west Asia (Barlow et al. 2005; Barlow 2012). It is thus inferred that the BSISO may play a role in the interdecadal change in southern China summer rainfall around 1992/1993.

To quantitatively assess the extent to which the interdecadal change of summer rainfall is influenced by the BSISO, a quantitative equation developed by Yoo et al. (2011, 2012a, b) is used in this subsection, which can be written as:

$$\left(\overline{A_2}-\overline{A_1}\right)_{BSISO}(\tau)=\frac{\sum_{i=1}^{8}\Delta A_{2,i}(\tau)N_{2,i}}{N}-\frac{\sum_{i=1}^{8}\Delta A_{1,i}(\tau)N_{1,i}}{N} \quad (1)$$

where A is the summer rainfall, N the total number of days in 1983–1992 (for brevity, P1) and 1993–2002 (for brevity, P2), which equals to 920, τ the lag day. An overbar means the time average and subscripts "1" and "2" denote P1 and P2, respectively. $\Delta A_{m,i}$ (τ), where $m = 1, 2$, indicates intraseasonal rainfall anomalies at τ day lag associated with phase i of the BSISO in P_m. $N_{m,i}$, where m = 1, 2, represents the number of active BSISO days over phase i in P_m. The left-hand side (lhs) of the Eq. (1) indicates the interdecadal change of summer rainfall induced by the BSISO (for brevity, BSISO-induced rainfall change). The first (second) term on right-hand side (rhs) of the Eq. (1) represents the product of lagged composite intraseasonal rainfall anomalies associated with BSISO phase i and

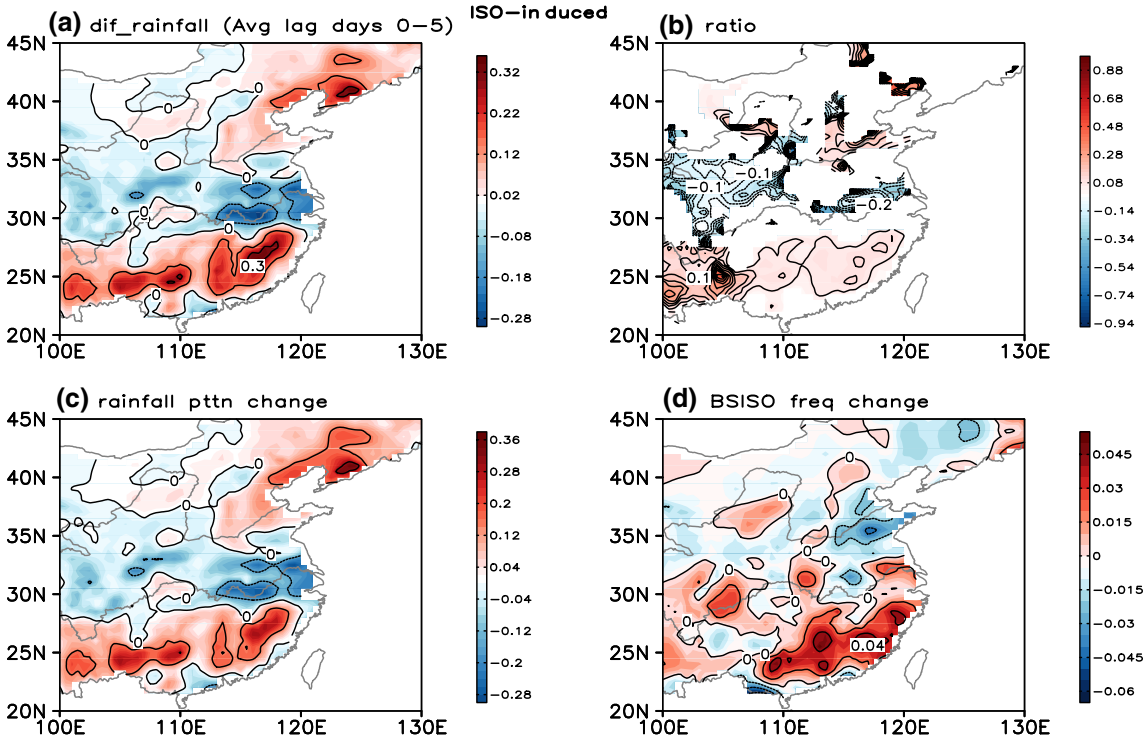

Fig. 5 **a** Spatial pattern of total interdecadal change of eastern China summer rainfall induced by the BSISO averaged over day 0 to lag 5 days (lhs of the Eq. 2). **b** The ratio between panel (**a**) and the observed interdecadal rainfall change (Fig. 3). BSISO-induced rainfall change due to (**c**) changes in spatial pattern of intraseasonal rainfall anomalies associated with BSISO phases (rainfall pattern change, first term on the rhs of the Eq. 2) and (**d**) changes in active frequency of BSISO phases (BSISO frequency change, second term on the rhs of the Eq. 2), averaged over day 0 to lag 5 days, summed over all eight BSISO phases. The contour interval of (**a**) and (**c**) is 0.15 mm day^{-1} while of (**d**) is 0.02 mm day^{-1}

the frequency of corresponding active phase in P1 (P2), summed over eight BSISO phases. It needs to be mentioned here that only active BSISO events (amplitude exceeding 1.5) would be concerned when conducting the above analysis. Decomposing $\Delta A_{m,i}$ and $N_{m,i}$ as $\Delta A_{m,i} = \Delta[A]_i + \Delta A^*_{m,i}$ and $N_{m,i} = [N]_i + N^*_{m,i}$respectively, where a square bracket indicates an time average over the period of 1983–2002, an asterisk denotes a deviation from the aforementioned average, Eq. (1) could be rewritten as:

$$\left(\overline{A_2} - \overline{A_1}\right)_{BSISO}(\tau) = \sum_{m=1}^{3} R_{\mathrm{m}}$$

where

$$R_1 = \frac{\sum_{i=1}^{8} \Delta A^*_{2,i}(\tau)[N]_i}{N} - \frac{\sum_{i=1}^{8} \Delta A^*_{1,i}(\tau)[N]_i}{N}$$
$$R_2 = \frac{\sum_{i=1}^{8} \Delta[A]_i(\tau)N^*_{2,i}}{N} - \frac{\sum_{i=1}^{8} \Delta[A]_i(\tau)N^*_{1,i}}{N} \quad (2)$$
$$R_3 = \frac{\sum_{i=1}^{8} \Delta A^*_{2,i}(\tau)N^*_{2,i}}{N} - \frac{\sum_{i=1}^{8} \Delta A^*_{1,i}(\tau)N^*_{1,i}}{N}$$

BSISO-induced rainfall change (lhs of Eqs. 1 and 2) could thus be explained by (1) interdecadal changes in spatial pattern of intraseasonal rainfall anomalies associated with each BSISO phase (R_1, for brevity, rainfall pattern change), (2) interdecadal changes in frequency of each active BSISO phase (R_2, BSISO frequency change) and (3) nonlinear influence comes from both rainfall pattern change and BSISO frequency change which is negligible (R_3).

It is readily seen that the spatial pattern of BSISO-induced rainfall change (Fig. 5a) averaged over 0 day to lag 5 days bears striking similarity to Fig. 3, especially over southern China. The above lag period is chosen to derive direct and steady rainfall changes associated with the BSISO. The ratio between BSISO-induced rainfall change (Fig. 5a) and observed interdecadal change in rainfall (Fig. 3, for brevity, interdecadal rainfall change) shows that changes in rainfall over southern China partially result from changes induced by the BSISO with an averaged ratio of about 17.4%. A closer observation into Fig. 5c, d reveals a dominant role of rainfall pattern change in the BSISO-induced rainfall change and a relatively smaller contribution of BSISO frequency change. Specifically, the spatial structure and magnitude of rainfall pattern change are nearly the same as the BSISO-induced rainfall change. The BSISO frequency change, albeit with small value, also contributes to the increased rainfall over southern China.

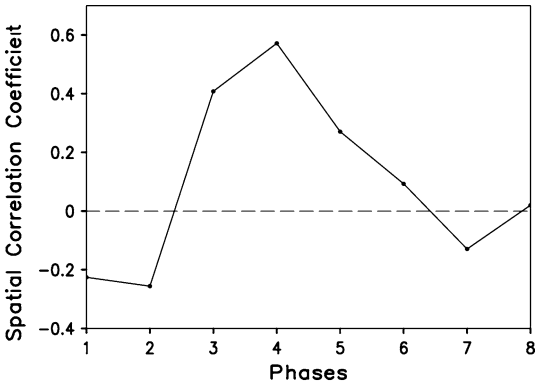

Fig. 6 Spatial correlation coefficient between interdecadal rainfall change associated with rainfall pattern change averaged over southern China (Fig. 5c, 100°–125°E, 20°–30°N) and rainfall pattern change associated with each BSISO phase (R_1 in Eq. 2 over southern China). The higher positive value is, the higher similarity of two spatial fields is expected

4.2.1 Impacts of rainfall pattern change

In previous subsection, a quantitative equation is used to calculate the BSISO-induced rainfall change in association with the rainfall pattern change and the BSISO frequency change. In this subsection and next subsection, specific impacts of rainfall pattern change and BSISO frequency change on interdecadal changes in southern China summer rainfall around 1992/1993 would be examined, respectively.

The summation of rainfall pattern change associated with eight phases of the BSISO has been proved to have prominent contributions to the interdecadal rainfall change in last subsection. To inspect relative role of each BSISO phase in the interdecadal rainfall change over southern China, spatial correlation coefficient is calculated between the total rainfall pattern change over southern China (Fig. 5c, 100°–125°E, 20°–30°N) and rainfall pattern change associated with each BSISO phase, and the result is shown in Fig. 6. The dominant role of phase 4 could be readily distinguished from other phases since the spatial correlation coefficient is approximately up to 0.6. The relative importance of phases 3 and 5 is also exposed with a correlation coefficient of around 0.4 and 0.25, respectively.

To analyze why the spatial patterns of intraseasonal summer rainfall anomalies over southern China associated with phases 3–5 of the BSISO experience interdecadal change around 1992/1993, anomalous OLR, 850 hPa horizontal wind, 850 hPa divergence and rainfall associated with BSISO phases 3–5 over P1, P2, and P2 minus P1 are displayed in Figs. 7, 8 and 9. In P1, the composite OLR of active BSISO events associated with phase 3 (Fig. 7a) represents enhanced convection over the northern IO north of the equator and weakened convection over the northern SCS. Corresponding to above spatial pattern of anomalous OLR, significant easterly winds could be identified over the southern SCS as a Kelvin wave response to anomalous convection over the northern IO. Meanwhile, an anomalous anticyclone is observed over the northern SCS (Fig. 7b). Controlled by this anomalous anticyclone, precipitation over southern China is decreased (Fig. 7c). In P2, the strengthened convection associated with phase 3 of the BSISO over the IO extends southward towards Eastern IO to the south of the equator and eastward towards the Maritime Continent; meanwhile, positive OLR anomalies around the Philippines becomes weaker (Fig. 7d). As a result, the easterlies associated with the negative OLR anomalies shift eastward and the anticyclone accompanied by positive OLR anomalies over the SCS is weakened. Hence the anomalous anticyclone over the northern SCS attenuates and moves southeastward in P2 (Fig. 7e). This causes the southward movement of above normal rainfall band over the Yangtze River region towards southern China (Fig. 7f). The differences between P2 and P1 (Fig. 7g) reinforce the fact that negative OLR anomalies over the IO associated with phase 3 of the BSISO stretch towards Eastern IO to the south of the equator and the Maritime Continent significantly. Corresponding to changes in spatial pattern of OLR anomalies, horizontal winds and divergence at lower level also changed, which further lead to changes in southern China summer rainfall (Fig. 7h, i).

The spatial structure of anomalous OLR associated with phase 4 of the BSISO in P1 is presented in Fig. 8a. Two elongated convective bands tilting from northwest to southeast with opposite signs could be found over the entire regions of the northern IO and the SCS. In response to the anomalous convection over the northern SCS, an anomalous anticyclone could be identified centered at 115°E (Fig. 8b). Influenced by this anomalous anticyclone is a dipole pattern of anomalous precipitation in China with the above-normal rainfall band located over the Yangtze River region and below-normal rainfall over southern China (Fig. 8c). In P2, the enhanced convective band breaks up into two centers with one anchored over the Arabian Sea and the other over the maritime continent (Fig. 8d). The main difference in OLR anomalies between P2 and P1 is the eastward shift of the strengthened convection from the southern SCS (west of 120°E) to the maritime continent (east of 120°E). As a result of changes in spatial pattern of anomalous convection, the main part of anomalous anticyclone would be partly offset by the anomalous cyclone induced by the enhanced convection over the maritime continent, which further results in the eastward retreat of the SCS anticyclone (Fig. 8e). The eastward retreat of the anomalous anticyclone hence leads to the southward intrusion of above-normal rainfall towards southern China (Fig. 8f). The above changes in spatial pattern of

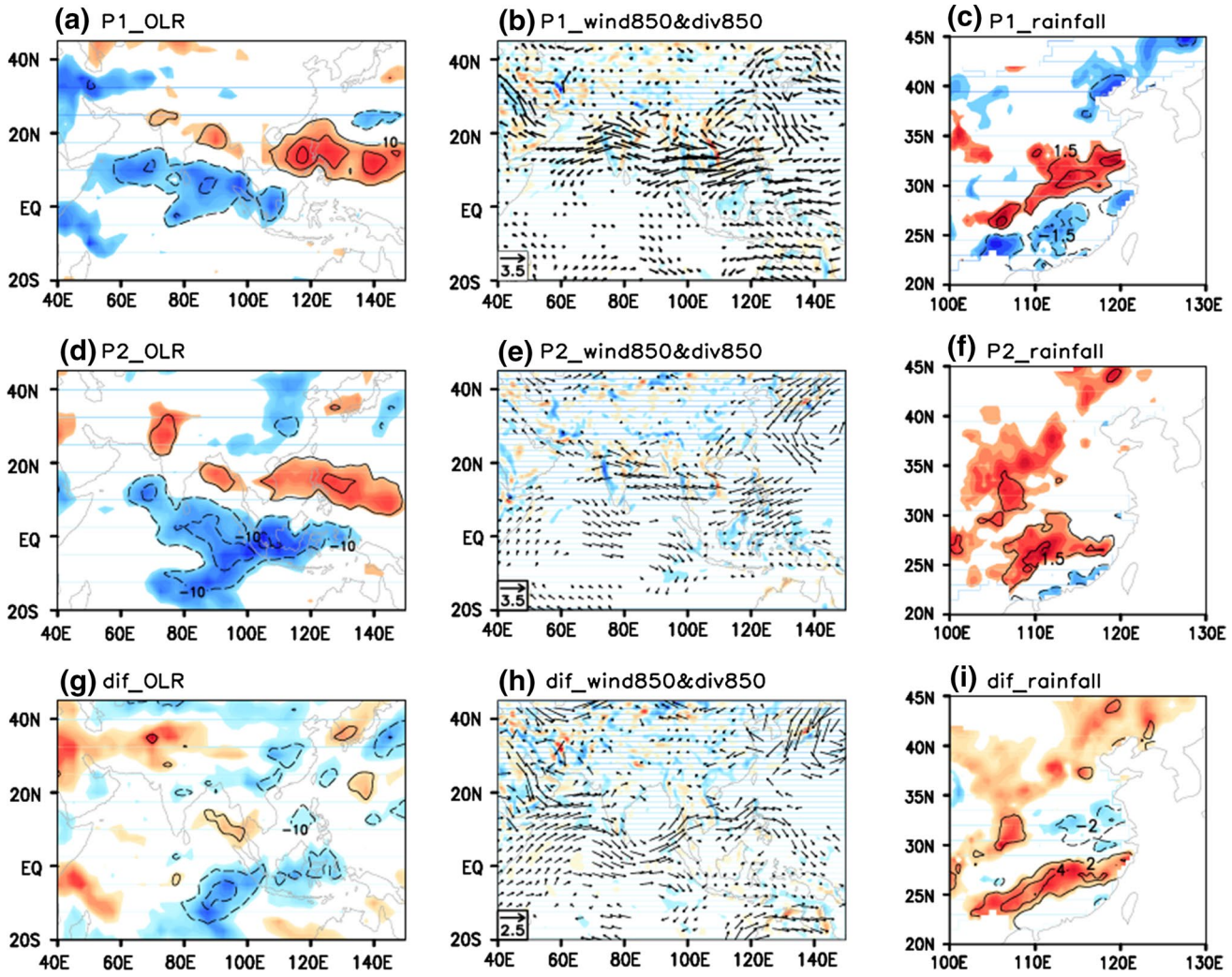

Fig. 7 *Left column* composite outgoing longwave radiation (OLR) anomalies (contour interval: 10 W m^{-2}) at day 0. *Middle column* composite horizontal wind (vector, unit: m s^{-1}) and divergence (shaded, interval: 0.5 × 10^{-6} s^{-1}) anomalies at 850 hPa (only values exceeding the 95% confidence level are plotted for both *shading* and vectors). *Right column* composite rainfall anomalies (contour interval is 1.5 mm day^{-1} for (**c**) and (**f**), 2 mm day^{-1} for (**i**)) averaged over day 0 to lag 5 days associated with phase 3 of the BSISO. **a**–**c** for P1 (1983–1992), **d**–**f** for P2 (1993–2002) and **g**–**i** P2 minus P1. The zero contours are not displayed in all plots. The *shadings* in (**a**), (**c**), (**d**), (**f**), (**g**), (**i**) indicate significant values exceeding the 95% confidence level according to the Student *t* test

precipitation from dipole pattern to monopole pattern result in the enhanced rainfall over southern China (Fig. 8i).

The changes in the spatial structure of anomalous OLR associated with phase 5 of the BSISO bears not only some similarities to that of phase 4, i.e., anomalous convection over the WP presented in P2 but absented in P1, but also some differences. The aforementioned anomalous convection develops in situ in the case of phase 5 instead of shifting from the SCS in the case of phase 4 (Figs. 8a, d, 9a, d). However, despite of difference in the formation of enhanced convection over the WP, the anomalous SCS anticyclone retreats and weakens in both cases and leads to a change in the spatial pattern of precipitation from dipole pattern to monopole pattern over South China (Figs. 8, 9).

The above changes in the spatial structure of OLR anomalies associated with BSISO phases allude to changes in BSISO tracks. To examine this speculation, the life cycle of the BSISO in P1 and P2 is presented individually in Figs. 10 and 11. BSISO events chosen to perform the composite analysis should be typical and persistent. In other words, the amplitude of the BSISO needs to exceed 1.5. What's more, an event needs to continuously develop from phase 1 to phase 8 without repetition. In P1 (Fig. 10), a salient negative OLR anomaly starts to appear in Eastern equatorial IO at phase 8. As time progresses, one branch continues propagating northward with the main body anchored north of the equator and another part moving eastward towards the southern SCS (phases 1–4). When the

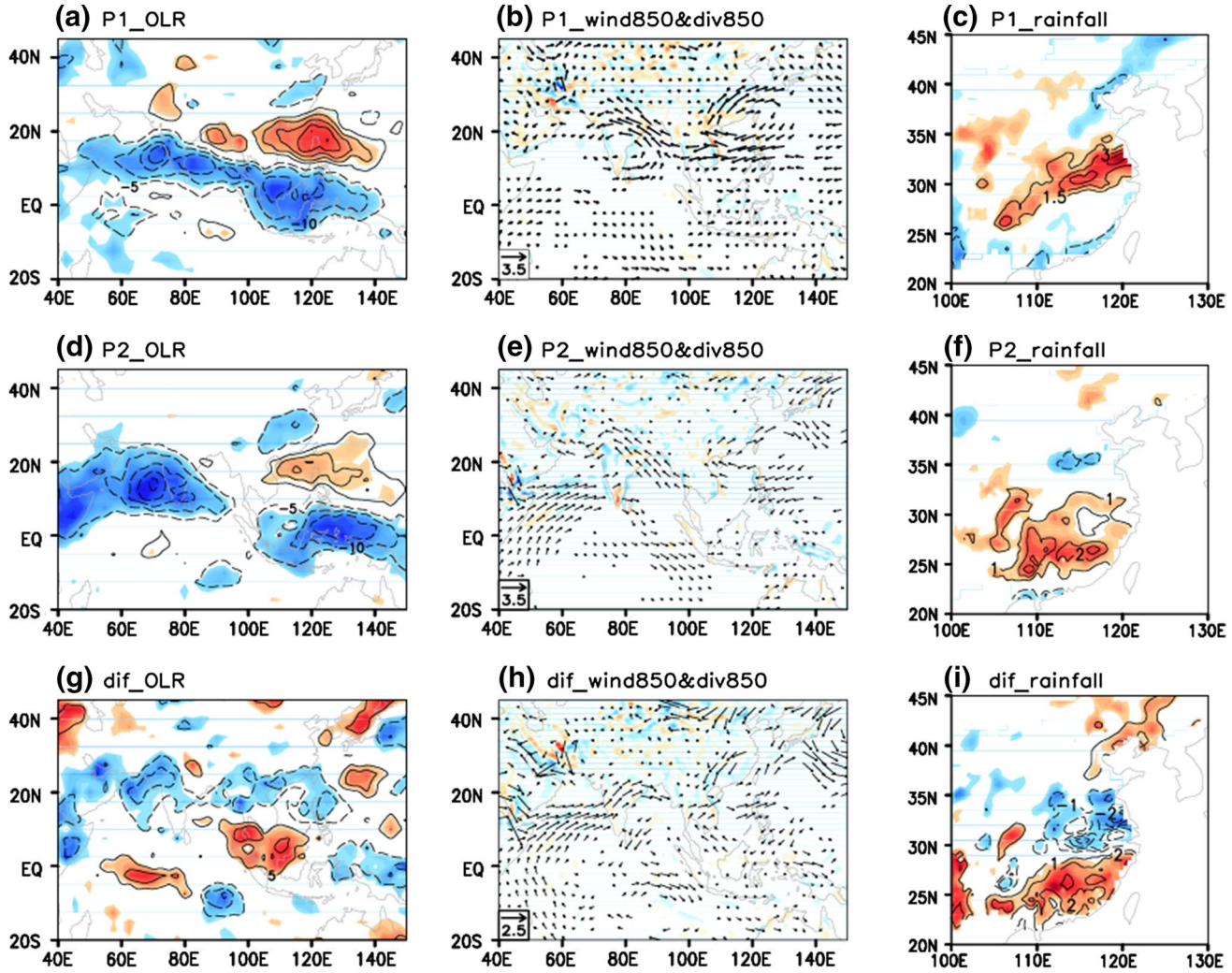

Fig. 8 Same as Fig. 7, but for composite anomalies associated with phase 4 of the BSISO. The contour interval is 5 W m^{-2} for (**a**), (**d**), (**g**), 1.5 mm day^{-1} for (**c**), and 1 mm day^{-1} for (**f**) and (**i**)

former branch reaches the Arabian Sea and the Bay of Bengal, it stays in situ and weakens rapidly (phases 5–7). In contrast, after reaching the southern SCS, the latter branch turns its direction of propagation from eastward to northward. It keeps moving towards the northern SCS through phase 5 to phase 8 and weakens at phase 1. Generally, the propagation of the BSISO in P1 is characterized by northward and eastward movements over the IO and northward movement over the SCS.

Examination of the BSISO track in P2 (Fig. 11) yields some striking differences with that in P1. Anomalous convection located over the IO extends to the south of the equator in P2 especially at phase 3 while keeps staying north of the equator in P1. Northward and northwestward movements of convective anomalies over the WP (including the SCS) are all appreciated in P2 instead of sole northward movement of anomalous convection discerned over the SCS in P1. The enhanced activity of northwestward-moving intraseasonal anomalies from the equatorial WP has been pointed out in Kajikawa and Wang (2012). According to their study, the strengthened northwestward movement of intraseasonal anomalies should be attributed to the sea surface warming over the WP. In light of above observed interdecadal changes in BSISO tracks, especially the prominent differences in phases 3–5 of the BSISO (manifested by spatial correlation analysis that phases 3–5 have smallest correlation between two periods, figure not shown), the spatial pattern of rainfall over southern China associated with phases 3–5 changed accordingly.

4.2.2 Impacts of BSISO frequency change

In above subsection, the causes of rainfall pattern change and its impact on the interdecadal change of southern

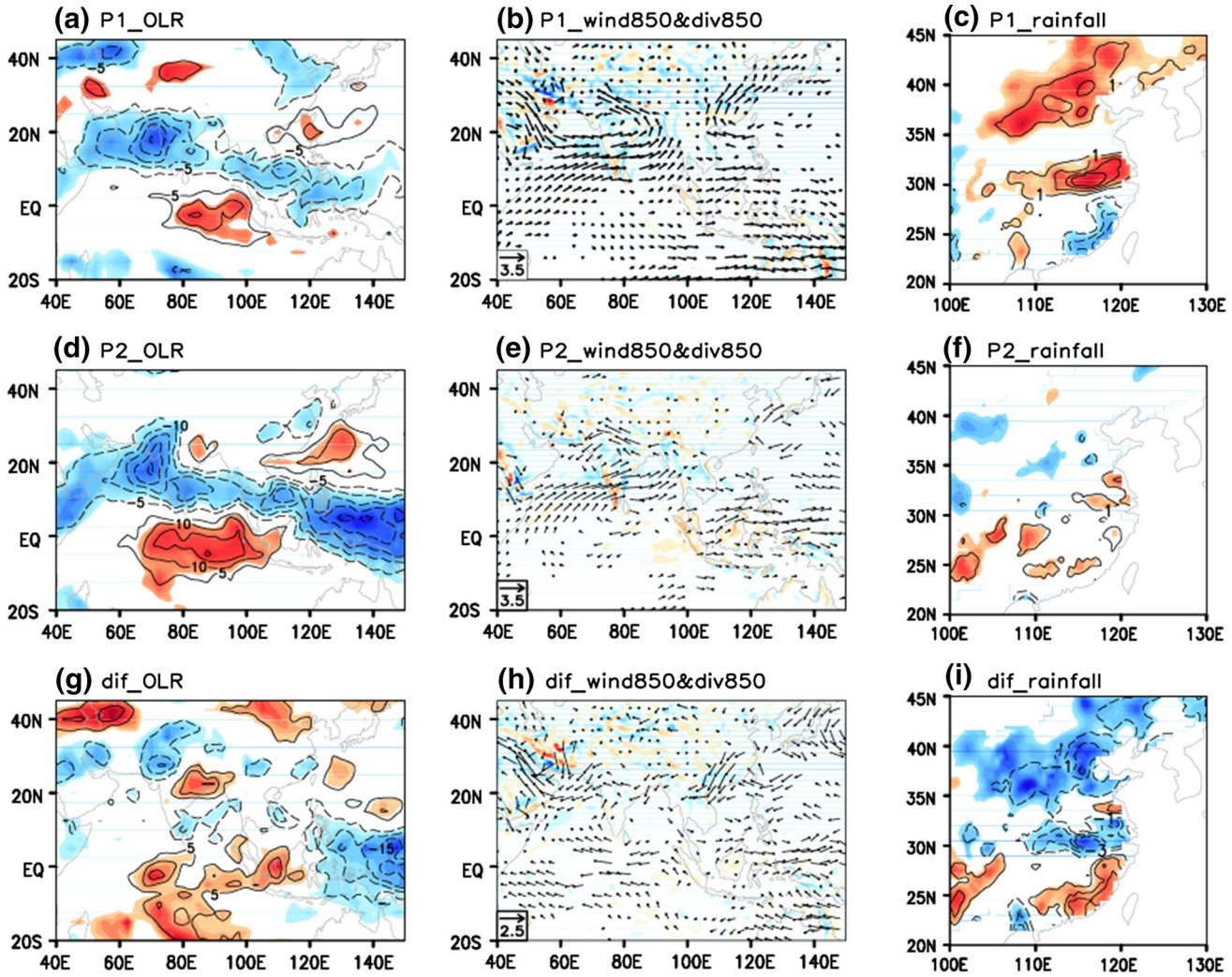

Fig. 9 Same as Fig. 7, but for composite anomalies associated with phase 5 of the BSISO. The contour interval is 5 W m^{-2} for (**a**), (**d**), (**g**), and 1 mm day^{-1} for (**c**), (**f**), (**i**)

China summer rainfall around 1992/1993 were analyzed. In this subsection, considering the fact that BSISO frequency change could also cast influence on the changes in rainfall over southern China, special attention would be given to the plausible reasons for the interdecadal change in the BSISO frequency and the possible impact on the interdecadal change in southern China summer rainfall.

To examine how changes in the frequency of BSISO phases contribute to the interdecadal rainfall change, the spatial correlation coefficient is recalculated between the BSISO frequency change related to each BSISO phase and the total rainfall decadal change associated with change in occurrence frequency of BSISO averaged over southern China (100°–125°E, 20°–30°N, Fig. 5d), which is presented in Fig. 12. The result suggests a prominent role of phase 1 and phase 8. The spatial patterns of precipitation change associated with phases 1 and 8 correspond to increased rainfall over southern China and decreased rainfall north of it (Fig. 13).

A comparison of the absolute frequency of each BSISO phase, $\frac{N_i}{N_{total}}$, where N_i, i = 1 to 8, refers to the number of days of active BSISO phase i, and N_{total} indicates the total number of days in P1 (P2) which is a constant number (920) for P1 (blue bars) and P2 (red bars), is shown in Fig. 14. Along with the absolute frequency of BSISO phases is the relative frequency of each BSISO phase, $\frac{N_i}{N_{BSISO}}$, where N_{BSISO} represents the number of days of active BSISO events in P1 (210 days) and P2 (284 days). The absolute frequency of each BSISO phase for P1 and P2 is compared to assess the interdecadal change of occurrence of each BSISO phase. The relative frequency between each phase is compared to distinguish changes in occurrence among BSISO phases. According to changes in the absolute frequency of each BSISO phase, there exists a notable

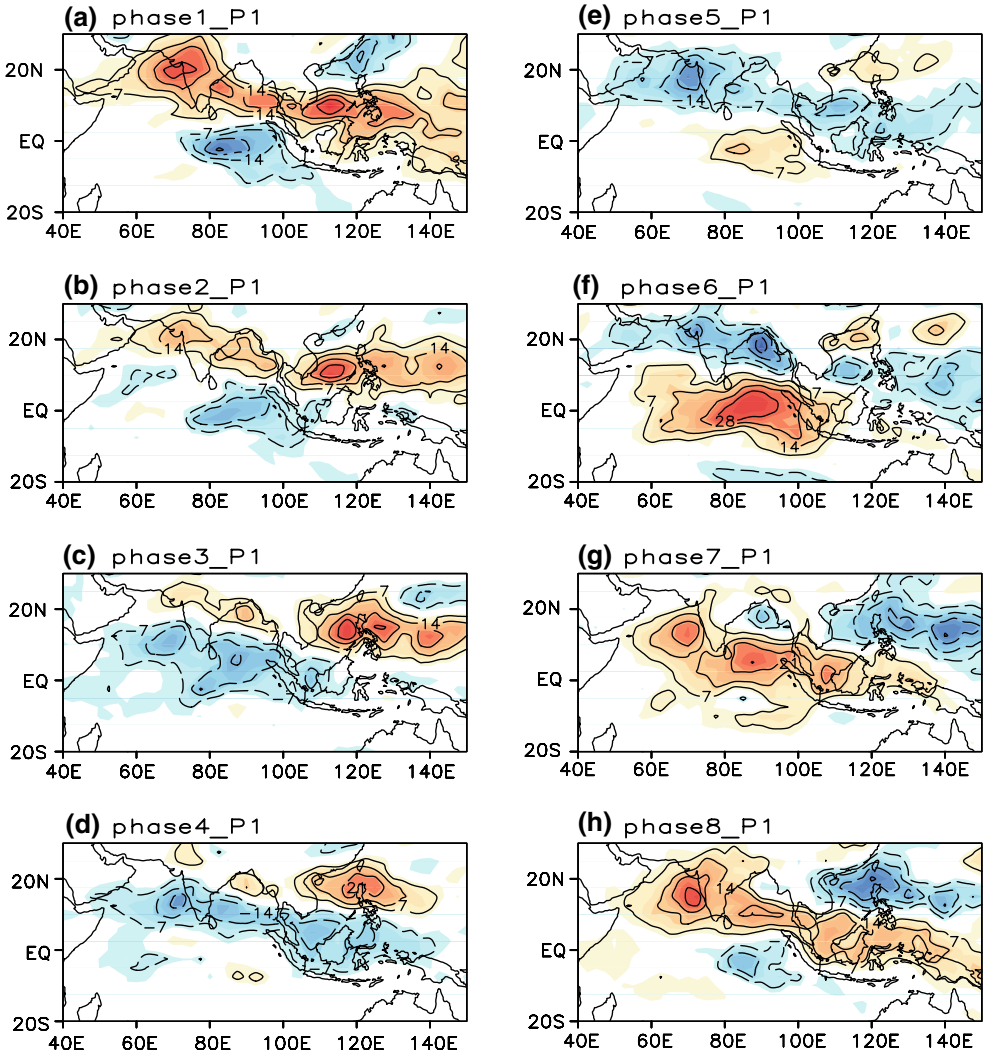

Fig. 10 Phase-composite life cycle of the BSISO mode in P1. The contours represent low-frequency OLR anomalies with the interval of 7 W m^{-2} (zero contour is omitted). Significant values exceeding the 99% confidence level according to the *t* test are shaded

increase of occurrence for all phases in P2. This interdecadal change of absolute frequency of BSISO phases should be ascribed to the intensification of anomalous convection rather than the variation in the length of period since averaged amplitude of each BSISO phase in P2 is strikingly larger than its counterpart in P1 but the averaged period of the BSISO in P2 (43 days) is nearly the same as it in P1 (40 days). By contrast, changes in the relative frequency of each BSISO phase are not in the same paces. Generally, phases 1, 6, 7 and 8 show remarkable increases while phases 2–5 exhibit prominent decreases in relative frequency. This indicates that the relative occurrence of phases 2–5 is reduced among all BSISO phases in P2 while the relative occurrence of the rest increases.

The above phenomena suggest some changes in the frequency of occurrence of the BSISO. Due to the intensification of anomalous convection in P2, occurrence frequency of all active BSISO phases increased since there are more numbers of days when BSISO amplitude exceeds the value of 1.5 in P2. Although the occurrence frequency of active BSISO phases increased in P2, intraseasonal convection anomalies are more likely to stay over the eastern North Pacific, the equatorial IO and WNP, which belong to phases 1, 6, 7, 8, rather than the Bay of Bengal, India, and the Maritime Continent, which belong to phases 2–5. Among all BSISO phases, phase 1 and phase 8 are of great concern in this study since they made positive contributions to the interdecadal change of southern China summer rainfall as previously pointed out. It is found that the absolute frequency and relative frequency of phases 1, 8 have all increased in P2. Coupled with their corresponding anomalous rainfall pattern (Fig. 13), the increased frequency of occurrence of phases 1, 8 results in the increased occurrence of an anomalous "+ −" pattern of precipitation

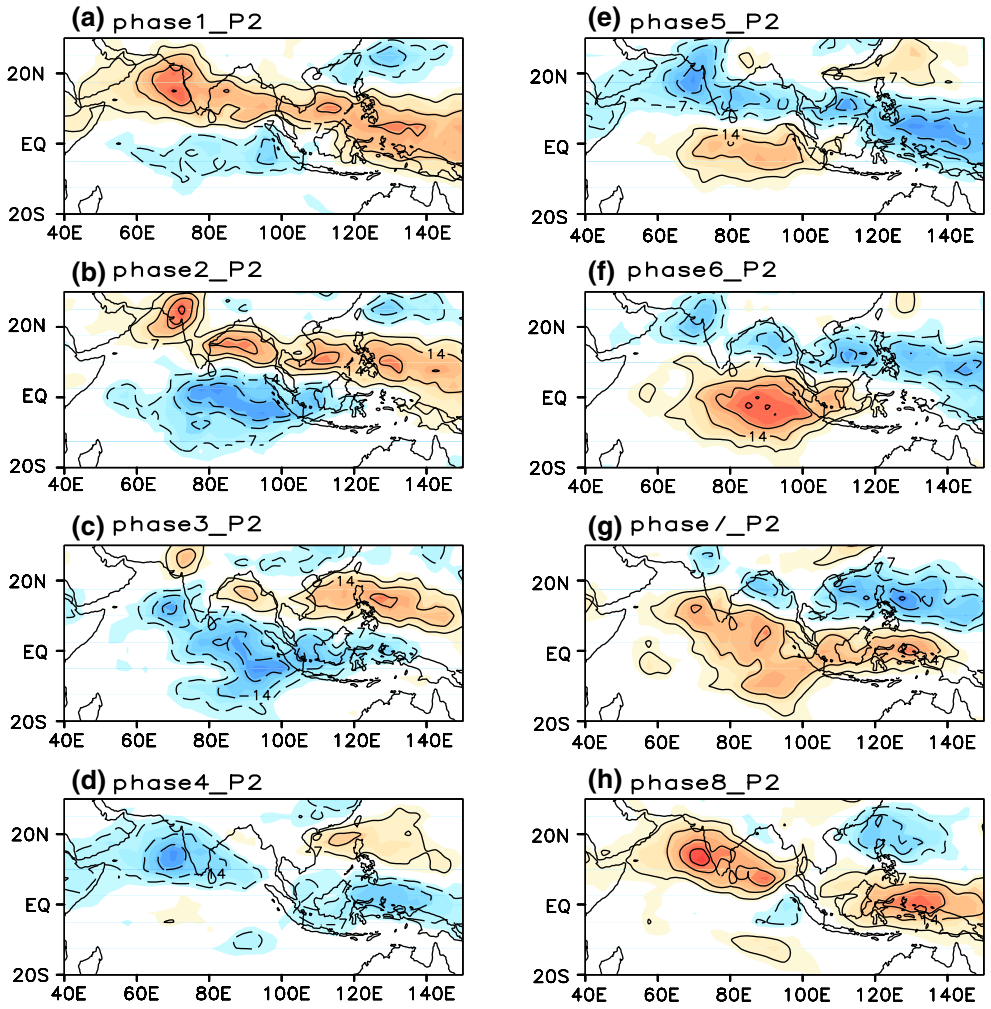

Fig. 11 Same as Fig. 10, but in P2

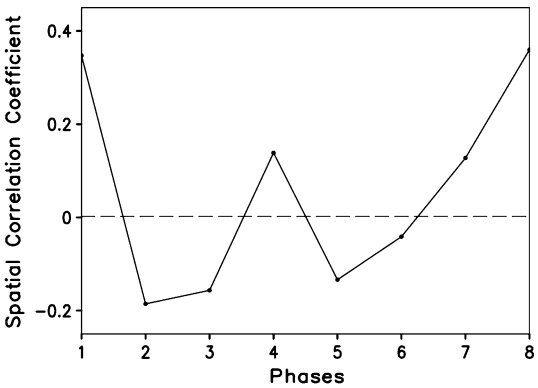

Fig. 12 Spatial correlation coefficient between interdecadal rainfall change associated with change in occurrence frequency of the BSISO averaged over southern China (Fig. 5d, 100°–125°E, 20°–30°N) and BSISO frequency change over southern China associated with each BSISO phase (R_2 in Eq. 2)

in P2, which further leads to an increase in southern China summer rainfall as an integral effect.

To explore the plausible reasons for changes in the BSISO track and occurrence frequency, 10-year differences in atmospheric circulation and sea surface temperature (SST) are displayed in Fig. 15. Figure 15a shows significant anomalous surface easterlies blowing from the SCS to the northern IO, superimposed on the climatological westerlies, leading to a wind speed decrease in the northern IO, the SCS and WNP. The decrease in surface wind speed would suppress the evaporation and hence favor the sea surface warming. Indeed, the SST in the WNP and SCS increased strikingly with an averaged warming of 0.2 °C. The SST in the northern IO also increased albeit with less significance (Fig. 15b). The above warming in the SCS, WNP and the northern IO would enhance the activities of intraseasonal convection (increased absolute frequency of

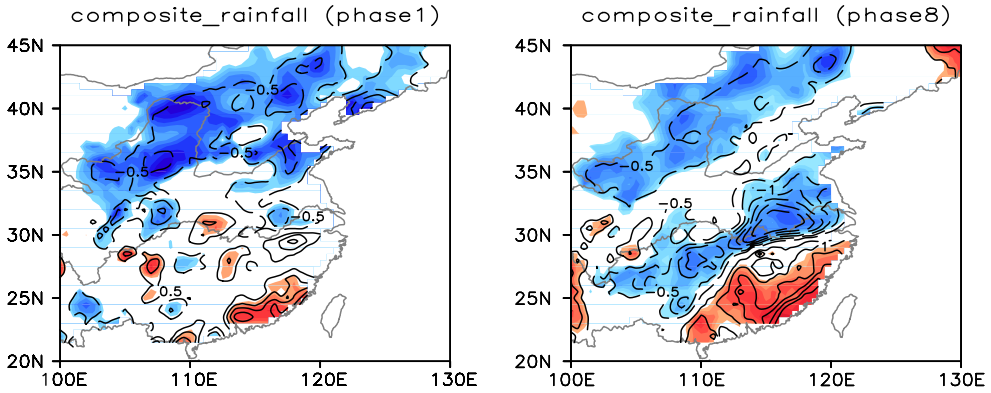

Fig. 13 Climatological Composite rainfall anomalies averaged over lag day 0 to day 5 associated with (*left panel*) phase 1 and (*right panel*) phase 8 of the BSISO with the contour interval of 0.5 mm day^{-1}. Zero contour is omitted in both panels. The *shadings* represent significant values exceeding the 95% confidence level according to the Student *t* test

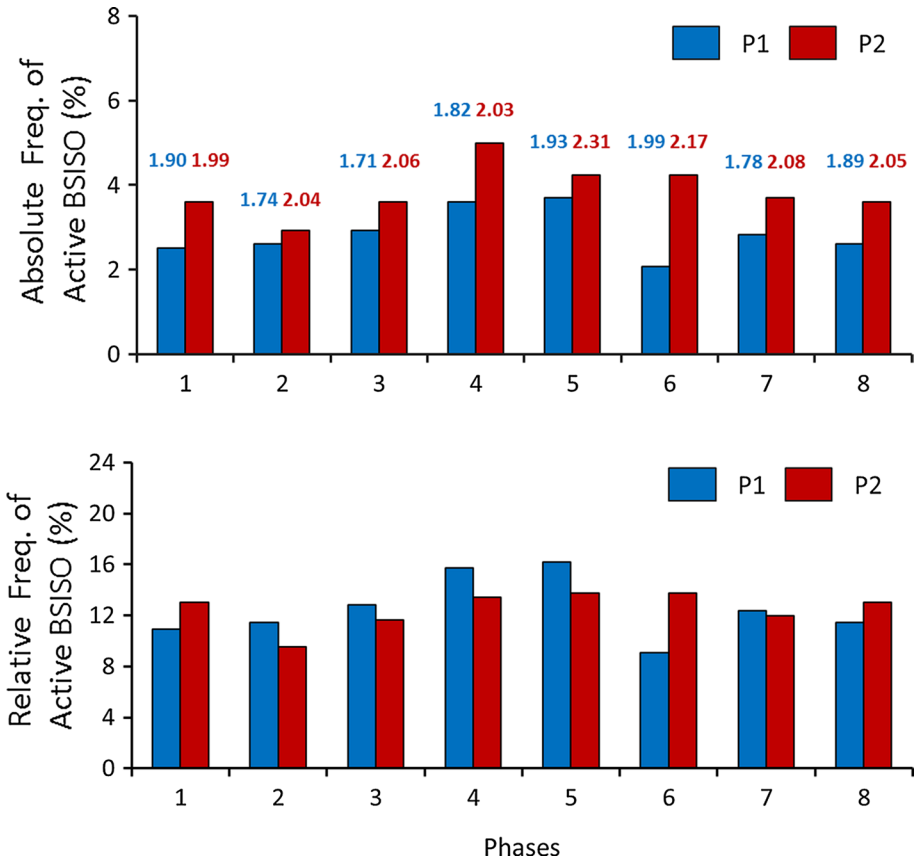

Fig. 14 Absolute (*top*) and relative (*bottom*) frequency (%) of BSISO phases. The specific meanings of absolute and relative frequency are explained in the article. The *blue bars* are for P1 while the *red bars* for P2. The numbers *on top* of the bars *in top panel* represent the averaged amplitude of chosen BSISO events (*blue* for P1, *red* for P2). The days are included in both panels when the amplitude of the BSISO index exceeding 1.5

BSISO phases, Slingo et al. 1999; Arnold et al. 2013). Significant changes could also be detected in latent heat flux. Nonetheless, the increased SST in the WNP and the northern IO is not accompanied by significant increase in surface latent heat flux in situ; instead, the significant increase in surface latent heat flux appears in the equatorial IO and WP to the south of the increased SST (Fig. 15c). Similar feature can be seen in the 10-year difference of boundary level divergence (Fig. 15d), which shows anomalous convergence in the equatorial IO and WP. In view of the decadal change of spatial structure of the BSISO (BSISO track change) which is characterized by: (1) extension of convection over the IO to south of the equator in P2 (Figs. 10c, 11c) and (2) northwestward movement over the WP originated from the equatorial WP in P2 instead of northward movement originated from the southern SCS in P1

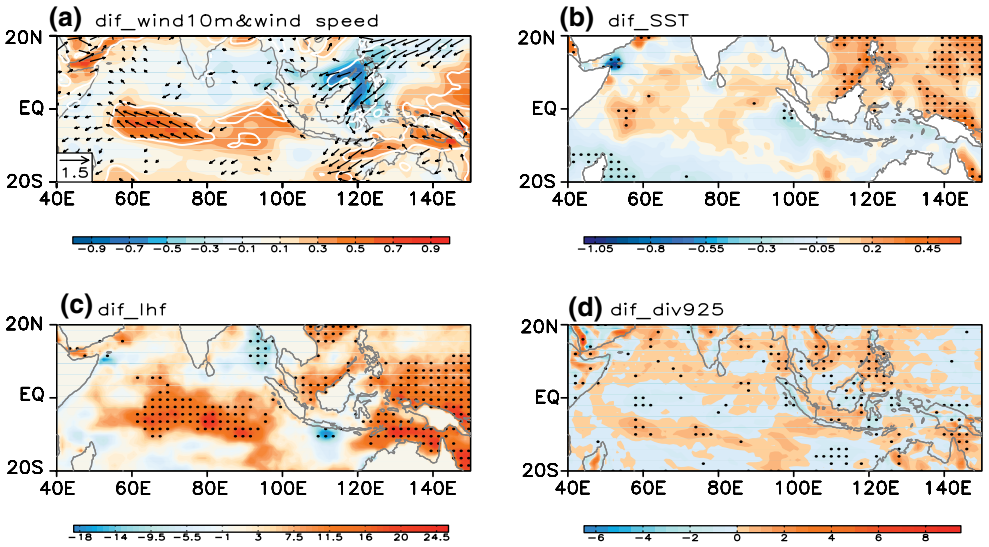

Fig. 15 10-year differences of JJA mean **a** surface wind (vector, unit: m s^{-1}) and wind speed (shaded, unit: m s^{-1}), **b** SST (°C), **c** latent heat flux (positive upward, unit: W m^{-2}) and **d** boundary level divergence (10^6 s^{-1}). The significant areas exceeding the 95% confidence level according to the Student *t* test are *encircled* by *white* contours in (**a**) while dotted in (**b**)–(**d**)

(Figs. 10e, 11e), the enhancement of upward surface latent heat flux and lower-level convergence in the equatorial IO and WP might facilitate the convection activities there and hence cause interdecadal change in the BSISO track.

5 Summary

Summer rainfall over southern China experienced a significant interdecadal increase around 1992/1993. In the present study, the mechanism for this interdecadal increase is investigated from perspective of intraseasonal timescale by means of diagnostic analysis. The principal findings presented in this article provide a supplementation to the knowledge of documented interdecadal change in summer rainfall around 1992/1993.

Analysis shows that the BSISO-induced rainfall change bears remarkable similarity to raw interdecadal rainfall change and explains approximately 17.4% of the latter over southern China. The BSISO-induced changes are primarily due to changes in rainfall pattern associated with the BSISO. In contrast, changes in the frequency of the active BSISO phases have a relatively smaller contribution.

Relative importance of the rainfall pattern change associated with each BSISO phase is analyzed. The results indicate that, among BSISO phases, changes in the rainfall pattern over southern China associated with phases 3–5 play crucial roles. The changes in OLR associated with phase 3 of the BSISO is characterized by a southward extension of anomalous OLR over the IO from north of the equator to the south of the equator and an eastward extension towards the Maritime Continent. As a result, the easterlies induced by anomalous OLR over the IO shift southeastward and the anomalous anticyclone over the northern SCS moves southeastward accordingly. Influenced by the interdecadal movement of the anomalous anticyclone, the above-normal rainfall band shifts from the Yangtze River region towards southern China, which leads to an increase in summer rainfall over South China. Different from changes in phase 3 of the BSISO, the changes in the OLR of phases 4–5 are characterized by the intensification of anomalous OLR over the equatorial WP, which result in the eastward retreat of the anomalous anticyclone over the SCS. As a result of above observed changes, the spatial pattern of summer rainfall over South China changed from dipole pattern to monopole pattern. The reasons for above changes in OLR are likely to be the changes in BSISO tracks. Apart from the northward and eastward movement documented in P1, the BSISO track in P2 displays other two directions of propagation, namely southward over the IO and northwestward over the WP.

The influence of the frequency of the active BSISO phases is also investigated. According to the results of spatial correlation coefficients, changes in frequency of phases 1 and 8 are found to be the most important. The absolute and relative frequency of phases 1 and 8 of the BSISO are both increased in P2. Hence, the number of days of occurrence of their corresponding anomalous "+ −" rainfall pattern would increase accordingly, which is favorable of enhanced southern China summer rainfall.

To examine the plausible reasons for the increased frequency of occurrence of phases 1 and 8 and the changes

in BSISO tracks, 10-year differences in surface wind, wind speed, SST, latent heat flux and boundary level divergence are analyzed. Based on discerned differences, sea surface warming over the WNP might be the catalyst for the increased frequency of the phase 8, which corresponds to strengthened convection over the WNP. By the same token, sea surface warming over the IO favored the increased frequency of the phase 1, which corresponds to the enhanced convection in situ. On the other hand, the increases in upward latent heat flux and boundary level convergence over the IO to the south of the equator and the equatorial WP might be the main reasons for interdecadal intensification of anomalous OLR over above regions, which result in the interdecadal change in BSISO tracks.

6 Discussion

This study suggests that increased SST over the WNP would result in enhanced occurrence frequency of BSISO over that region (i.e., phase 8). Similar finding was pointed out by Kajikawa and Wang (2012) that indicated that sea surface warming over the NWP would excite Rossby waves to west which favors low-level convergence and hence increases the possibility of convection activities. Li and Zhou (2014) also found the role of SST in BSISO activity. The negative zonal SST gradient between the tropical Pacific and IO would induce an anomalous inverse Walker-like circulation which results in an anomalous rising motion and boundary layer convergence over the northern SCS and hence increased occurrence of BSISO activity there. Although this study tries to explore potential mechanism of BSISO change resulting from mean state change around 1992/1993, a deeper understanding is needed with the help of the state of the art models, which calls for further study.

This study mainly focuses on the contribution of intraseasonal component to total decadal change of summer rainfall over southern China. However, the proposed impact of the BSISO rainfall change on the total rainfall change over southern China is relatively limited (Fig. 4b) that the BSISO rainfall change accounts for only around 10% of significant change in total rainfall. Therefore, other factors, e.g., high-frequency variation (2–8 day) which makes large percentage contribution (50%) to the total variance of summer rainfall over southern China (figure not shown), need to be investigated in future study.

The dominance of quasi-biweekly oscillation in southern China summer rainfall variation is rather weak in this study (Fig. 1), which is below the 90% confidence level. Some previous studies suggested a peak of quasi-biweekly oscillation (Yang et al. 2008, 2010; Chen and Sui 2010; Pan et al. 2013; Gao et al. 2016). We have conducted additional analysis to understand the reasons of relative weak peak of this oscillation period in Fig. 1. Our analysis shows that whether the peak in quasi-biweekly oscillation is significant is sensitive to the analysis period and months. For instance, when we extend the spectral analysis period to a longer period from 1983 to 2012, a significant peak of quasi-biweekly oscillation is detected (figure not shown). This is consistent with a recent intensification in quasi-biweekly oscillation in southern China summer rainfall (Chen et al. 2014a, b). On the other hand, when the spectral analysis is focused on June to July which is suggested to be dominated by quasi-biweekly oscillation (e.g., Yang et al. 2008) instead of JJA, a significant peak is found in 12–20 days as well. Therefore, the relative weak peak of quasi-biweekly oscillation in this study may be due to the dependence on the time periods and months.

When analyzing summer rainfall over East China, some previous studies separated summer into early (May and June) and late summer (July and August) according to the northward movement of rain belt and significant difference in atmospheric circulation between early and late summer (e.g., Wang et al. 2009a, b). Therefore, we investigated the difference in interdecadal change of summer rainfall over southern China between early and late summer (figure not shown). The results indicate that interdecadal increase over southern China in early summer is less significant and with a smaller spatial coverage than that in late summer. Other than that, the importance of intraseasonal component to the interdecadal increase over southern China is observed in both early and later summer cases. However, the EOF analysis for each month (May to August, figures not shown) suggests that the leading mode of precipitation in June, July and August bears similar spatial distribution and interdecadal change, i.e., they are all characterized by quasi-tripole pattern and their corresponding PC1s indicate decadal shift from below (above)-normal to above (below)-normal precipitation over southern China (Yangtze River region) at around 1992/1993. On the other hand, the EOF1 mode of precipitation in May not only differs a lot from JJA in terms of its dominant pattern, but also has different interdecadal variabilities. For instance, its PC1 suggests a decadal decrease in southern China rainfall at around 1992/1993, which is entirely opposite to the decadal change found in June to August. In light of this, it might be inappropriate to include May when analyzing documented decadal increase in southern China rainfall around 1992/1993.

Acknowledgements This research was jointly supported by National Natural Science Foundation of China (41530530), National Key Basic Research, Development Projects of China (2014CB953901) and State Key Laboratory of Severe Weather opening project. RW acknowledges the support of National Natural Science Foundation of China Grants (41275081 and 41475081).

References

Aldrian E (2008) Dominant factors of Jakarta's three largest floods. J Hidrosfir Indones 3:105–112

Arnold NP, Kuang Z, Tziperman E (2013) Enhanced MJO-like variability at high SST. J Clim 26(3):988–1001

Barlow M (2012) Africa and west Asia. In: Lau WK-M, Waliser DE (eds) Intraseasonal variability of the atmosphere–ocean climate system, 2nd edn. Springer, Berlin, pp 477–496

Barlow M, Wheeler M, Lyon B, Cullen H (2005) Modulation of daily precipitation over southwest Asia by the Madden–Julian oscillation. Mon Weather Rev 133:3579–3594

Chen G, Sui CH (2010) Characteristics and origin of quasi-biweekly oscillation over the western North Pacific during boreal summer. J Geophys Res 115:D14113. doi:10.1029/2009JD013389

Chen L, Zhu C, Wang W et al (2001) Analysis of the characteristics of 30–60 day low-frequency oscillation over Asia during 1998 SCSMEX. Adv Atmos Sci 18(4):623–638

Chen J, Wu R, Wen Z (2012) Contribution of South China Sea tropical cyclones to an increase in southern China summer rainfall around 1993. Adv Atmos Sci 29(3):585–598

Chen J, Wen Z, Wu R, Chen Z, Zhao P (2014a) Influences of northward propagating 25–90-day and quasi-biweekly oscillations on eastern China summer rainfall. Clim Dyn. doi:10.1007/s00382-014-2334-y

Chen Z, Wen Z, Wu R, Zhao P, Cao J (2014b) Influence of two types of El Niño on the East Asian climate during boreal summer: a numerical study. Clim Dyn 43:469–481

Dee DP, Uppala S (2009) Variational bias correction of satellite radiance data in the ERA-Interim reanalysis. Q J R Meteorol Soc 135(644):1830–1841. doi:10.1002/qj.493

Ding Y, Wang Z, Sun Y (2008) Inter-decadal variation of the summer precipitation in East China and its association with decreasing Asian summer monsoon. Part I: observed evidences. Int J Climatol 28(9):1139–1161. doi:10.1002/joc.1615

Duchon CE (1979) Lanczos filtering in one and 2 dimensions. J Appl Meteorol 18:1016–1022. doi:10.1175/1520-0450(1979)018<1016:LFIOAT>2.0.CO;2

Ferranti L, Palmer TN, Molteni F, Klinker E (1990) Tropical–extratropical interaction associated with the 30–60-day oscillation and its impact on medium and extended range prediction. J Atmos Sci 47:2177–2199

Gao J, Lin H, You L, Chen S (2016) Monitoring early-flood season intraseasonal oscillations and persistent heavy rainfall in South China. Clim Dyn. doi:10.1007/s00382-016-3045-3

Goswami BN (2012) South Asian monsoon. In: Lau WK-M, Waliser DE (eds) Intraseasonal variability of the atmosphere–ocean climate system, 2nd edn. Springer, Berlin, pp 21–72

He J, Lin H, Wu Z (2011) Another look at influences of the Madden–Julian oscillation on the wintertime East Asian weather. J Geophys Res 116:D03109. doi:10.1029/2010JD014787

Higgins RW, Mo KC (1997) Persistent North Pacific circulation anomalies and the tropical intraseasonal oscillation. J Clim 10:223–244

Hsu H-H (2012) East Asian monsoon. In: Lau WK-M, Waliser DE (eds) Intraseasonal variability of the atmosphere–ocean climate system, 2nd edn. Springer, Berlin, pp 73–110

Jeong J-H, Kim B-M, Ho C-H, Noh Y-H (2008) Systematic variation in wintertime precipitation in East Asia by MJO-induced extratropical vertical motion. J Clim 21:788–801

Jia X, Chen LJ, Ren FM, Li CY (2011) Impacts of the MJO on winter rainfall and circulation in China. Adv Atmos Sci 28:521–533. doi:10.1007/s00376-010-9118-z

Jiang X, Li T, Wang B (2004) Structures and mechanisms of the northward propagating boreal summer intraseasonal oscillation. J Clim 17:1022–1039

Kajikawa Y, Wang B (2012) Interdecadal change of the South China Sea summer monsoon onset. J Clim 25:3207–3218. doi:10.1175/JCLI-D-11-00207.1

Kajikawa Y, Yasunari T, Wang B (2009) Decadal change in intraseasonal variability over the South China Sea. Geophys Res Lett 36:L06810. doi:10.1029/2009gl037174

Kikuchi K, Wang B, Kajikawa Y (2012) Bimodal representation of the tropical intraseasonal oscillation. Clim Dyn 38:1989–2000. doi:10.1007/s00382-011-1159-1

Kwon M, Jhun JG, Ha KJ (2007) Decadal change in East Asian summer monsoon circulation in the mid-1990s. Geophys Res Lett 34:L21706. doi:10.1029/2007GL031977

Lau K-M, Chan P-H (1986) Aspects of the 40–50 day oscillation during the northern summer as inferred from outgoing longwave radiation. Mon Weather Rev 114:1354–1367

Lawrence DM, Webster PJ (2001) Interannual variations of the intraseasonal oscillation in the South Asian summer monsoon region. J Clim 14:2910–2922

Lawrence DM, Webster PJ (2002) The boreal summer intraseasonal oscillation: relationship between northward and eastward movement of convection. J Atmos Sci 59:1593–1606

Lee S, Feldstein S, Pollard D, White T (2011a) Do planetary wave dynamics contribute to equable climates? J Clim 24:2391–2404

Lee S, Gong T, Johnson N, Feldstein S, Pollard D (2011b) On the possible link between tropical convection and the Northern Hemisphere Arctic surface air temperature change between 1958 and 2001. J Clim 24:4350–4367

Li CY, Zhou W (2014) Interdecadal change in South China Sea tropical cyclone frequency in association with zonal sea surface temperature gradient. J Clim 27:5468–5480

Madden RA, Julian PR (1971) Detection of a 40–50 day oscillation in the zonal wind in the tropical Pacific. J Atmos Sci 28:702–708

Madden RA, Julian PR (1972) Description of global-scale circulation cells in the tropics with a 40–50 day period. J Atmos Sci 29:1109–1123

Mao J, Chan JCL (2005) Intraseasonal variability of the South China Sea summer monsoon. J Clim 18(3):2388–2402

Mutai CC, Ward MN (2000) East African rainfall and the tropical circulation/convection on intraseasonal to interannual timescales. J Clim 13:3915–3939

Ning L, Qian Y (2009) Interdecadal change in extreme precipitation over South China and its mechanism. Adv Atmos Sci 26(1):109–118. doi:10.1007/s00376-009-0109-x

North GR, Bell TL, Cahalan RF, Moeng FJ (1982) Sampling errors in the estimation of empirical orthogonal functions. Mon Weather Rev 110:699–706

Pan WJ, Mao JY, Wu GX (2013) Characteristics and mechanism of the 10–20-day oscillation of spring rainfall over southern China. J Clim 26:5072–5087. doi:10.1175/JCLI-D-12-00618.1

Qian W, Qin A (2008) Precipitation division and climate shift in China from 1960 to 2000. Theor Appl Climatol 93:1–17. doi:10.1007/s00704-007-0330-4

Slingo JM, Rowell DP, Sperber KR, Nortley F (1999) On the predictability of the interannual behaviour of the Madden–Julian oscillation and its relationship with el Niño. Q J R Meteorol Soc 125:583–609. doi:10.1002/qj.49712555411

Tangang FT, Juneng L, Salimun E, Vinayachandran PN, Seng YK, Reason CJC, Behera SK, Yasunari T (2008) On the roles of the northeast cold surge, the Borneo vortex, the Madden–Julian oscillation, and the Indian Ocean dipole during the extreme 2006/2007 flood in southern peninsular Malaysia. Geophys Res Lett 35:L14S07. doi:10.1029/2008GL033429

Wang B, Rui H (1990) Synoptic climatology of transient tropical intraseasonal convective anomalies: 1975–1985. Meteorol Atmos Phys 44:43–61

Wang B, Xie X (1997) A model for the boreal summer intraseasonal oscillation. J Atmos Sci 54:72–86

Wang B, Xu X (1997) Northern hemisphere summer monsoon singularities and climatological intraseasonal oscillation. J Clim 10:1071–1085

Wang B, Huang F, Wu Z, Yang J, Fu X, Kikuchi K (2009a) Multi-scale climate variability of the South China Sea monsoon: a review. Dyn Atmos Ocean 47:15–37. doi:10.1016/j.dynatmoce.2008.09.004

Wang B, Liu J, Yang J, Zhou T, Wu Z (2009b) Distinct principal modes of early and late summer rainfall anomalies in East Asia. J Clim 22:3864–3875

Wheeler MC, Hendon HH (2004) An all-season real-time multivariate MJO index: development of an index for monitoring and prediction. Mon Weather Rev 122:1917–1932

Wu R, Wen Z, Yang S, Li Y (2010) An interdecadal change in southern China summer rainfall around 1992/1993. J Clim 23:2389–2403. doi:10.1175/2009JCLI3336.1

Yamaura T, Kajikawa Y (2016) Decadal change in the boreal summer intraseasonal oscillation. Clim Dyn. doi:10.1007/s00382-016-3247-8

Yang H, Li C (2003) The relation between atmospheric intraseasonal oscillation and summer severe flood and drought in the Changjiang–Huaihe River basin. Adv Atmos Sci 20(4):540–553

Yang J, Wang B, Wang B (2008) Anticorrelated intensity change of the quasi-biweekly and 30–50-day oscillations over the South China Sea. Geophys Res Lett 35:L16702. doi:10.1029/2008GL034449

Yang J, Wang B, Wang B, Bao Q (2010) Biweekly and 21–30-day variations of the subtropical summer monsoon rainfall over the lower reach of the Yangtze River basin. J Clim 23:1146–1159

Yao C, Yang S, Qian W, Lin Z, Wen M (2008) Regional summer precipitation events on Asia and their changes in the past decades. J Geophys Res 113:D17107. doi:10.1029/2007JD009603

Yoo C, Feldstein S, Lee S (2011) The impact of the Madden–Julian Oscillation trend on the Arctic amplification of surface air temperature during the 1979–2008 boreal winter. Geophys Res Lett 38:L24804. doi:10.1029/2011GL049881

Yoo C, Lee S, Feldstein S (2012a) The impact of the Madden–Julian oscillation trend on the Antarctic warming during the 1979–2008 austral winter. Atmos Sci Lett 13:194–199. doi:10.1002/asl.379

Yoo C, Lee S, Feldstein S (2012b) Mechanisms of arctic surface air temperature change in response to the Madden–Julian oscillation. J Clim 25:5777–5790. doi:10.1002/asl.379

Zhang C (2013) Madden–Julian oscillation: bridging weather and climate. Bull Am Meteorol Soc 94:1849–1870. doi:10.1175/BAMS-D-12-00026.1

Zhang L, Wang B, Zeng Q (2009) Impacts of the Madden–Julian oscillation on summer rainfall in Southeast China. J Clim 22:201–216. doi:10.1175/2008JCLI1959.1

Zhou W, Li C, Chan JCL (2006) The interdecadal variations of the summer monsoon rainfall over South China. Meteorol Atmos Phys 93(3−4):165–175. doi:10.1007/s00703-006-0184-9

Zhu C, Nakazawa T, Li J, Chen L (2003) The 30–60 day intraseasonal oscillation over the western North Pacific Ocean and its impacts on summer flooding in China during 1998. Geophys Res Lett 30:1952. doi:10.1029/2003GL017817